Diagn Interv Radiol 2020; 26:370–376

PEDIATRIC RADIOLOGY

ORIGINAL ARTICLE

Hepatocyte-specific contrast-enhanced MRI findings of focal nodular hyperplasia-like nodules in the liver following chemotherapy in pediatric cancer patients

H. Nursun Özcan
Muşturay Karçaaltıncaba
Turgut Seber
Bilgehan Yalçın
Berna Oğuz
Canan Akyüz
Mithat Haliloğlu

PURPOSE
We aimed to assess the MRI findings and follow-up of multiple focal nodular hyperplasia (FNH)-like lesions in pediatric cancer patients diagnosed by imaging findings.

METHODS
We retrospectively analyzed clinical data and MRI examinations of 16 pediatric patients, who had been scanned using gadoxetate disodium (n=13) and gadobenate dimeglumine (n=3). Hepatic nodules were reviewed according to their number, size, contour, T1- and T2-weighted signal intensities, arterial, portal, delayed and hepatobiliary phase enhancement patterns. Follow-up images were evaluated for nodule size, number, and appearance.

RESULTS
All 16 patients received chemotherapy in due course. Time interval between the initial diagnosis of cancer and detection of the hepatic nodule was 2–14 years. Three patients had a single lesion, 13 patients had multiple nodules. The median size of the largest nodules was 19.5 mm (range, 8–41 mm). Among 16 patients that received hepatocyte-specific agents, FNH-like nodules appeared hyperintense in 11 and isointense in 5 on the hepatobiliary phase. During follow-up, increased number and size of the nodules were seen in 4 patients. The nodules showed growth between 6–15 mm.

CONCLUSION
Liver MRI using hepatocyte-specific agents is a significant imaging method for the diagnosis of FNH-like lesions, which can occur in a variety of diseases. Lesions can increase in size and number in pediatric patients.

Focal nodular hyperplasia (FNH) is uncommon in pediatric patients. It is usually seen as a single lesion, which is hypervascular on the arterial phase. FNH retains a hyperintense appearance or demonstrates isointensity with the normal liver parenchyma during the subsequent portal venous phase. Additionally, the central fibrotic scar retains contrast on delayed scans with gadolinium-based contrast agents (1). Recent articles also demonstrated that hyperintensity on hepatobiliary phase images using gadobenate dimeglumine (Gd-BOPTA) or gadoxetate disodium (Gd-EOB-DTPA) is an important imaging characteristic for FNH (1, 2).

FNH-like lesions have been described in cirrhotic livers as multiple regenerative nodules distributed throughout the liver, structurally and immunohistochemically resembling classical FNH seen in noncirrhotic livers (3). FNH-like nodules most likely occur as a consequence of hyperplastic response of the hepatic parenchyma due to alteration in the hepatic blood flow (4, 5). These nodules can sometimes be misdiagnosed as liver metastases in pediatric patients under chemotherapy. To avoid unnecessary invasive procedures, prompt imaging is crucial for the diagnosis of FNH-like nodules. In this situation, MRI using hepatocyte-specific contrast agents may be useful for the diagnosis of FNH-like nodules. FNH-like nodules are hypervascular on arterial phase images and they demonstrate hyperintensity on the hepatobiliary phase (1).

In the pertinent literature, majority of the previous reports demonstrated the clinical course, epidemiology, and pathogenesis of the FNH-like nodules (5–11). Likewise, there

From the Departments of Radiology (H.N.Ö. ✉ *drhnozcan@yahoo.com*, M.K., B.O., M.H.) and Pediatrics, Division of Pediatric Oncology (B.Y., C.A.), Hacettepe University School of Medicine, Ankara, Turkey; Department of Radiology (T.S.), Kayseri City Hospital, Kayseri, Turkey.

Received 16 August 2019; revision requested 16 September 2019; last revision received 03 November 2019; accepted 11 November 2019.

Published online 27 May 2020.

DOI 10.5152/dir.2019.19398

You may cite this article as: Özcan HN, Karçaaltıncaba M, Seber T, et al. Hepatocyte-specific contrast-enhanced MRI findings of focal nodular hyperplasia-like nodules in the liver following chemotherapy in pediatric cancer patients. Diagn Interv Radiol 2020; 26:370–376.

Table 1. MRI sequence parameters

Sequence	Plane	TR (ms)	TE (ms)	Flip angle	Fat saturation	Matrix	FOV (mm)	Slice thickness
TRUE-FISP	Coronal	4.3	2.1	60	-	416×512	284.4×350	4.5
T2 TSE	Axial	1350	92	160	-	256×256	355×355	6
T1 GRE in and out of phase	Axial	160	In phase:4.9 Out of phase:2.4	70	-	256×192	350×262	6
T2 TSE FS	Axial	3050	125	150	+	256×256	355×355	6
T1 3D GRE VIBE	Axial	5	2.4	10	+	320×240	355×266	3
T1 3D GRE VIBE hepatobiliary	Axial	5	2.4	30	+	320×240	355×266	3
Diffusion (b=50, 400, 800 s/mm^2)	Axial	6438	87	90	-	192×156	355×288	6

TR, repetition time; TE, echo time; FOV, field of view; TRUE-FISP, true fast imaging with steady state precession; TSE, turbo spin echo; GRE, gradient echo; FS, fat-saturated; 3D, three-dimensional; VIBE, volumetric interpolated breath-hold examination.

are several articles describing the computed tomography (CT) and MRI findings of FNH-like nodules (12–19). Herewith, the application of hepatocyte-specific agents in pediatric patients has not been assessed in many studies. Accordingly, in this study, we aimed to analyze the dynamic contrast-enhanced MRI findings of multiple FNH-like lesions using hepatocyte-specific agents in pediatric cancer patients including their follow-up.

Methods

Patients

This was a retrospective study approved by the local ethics committee (GO 18/839-14). Informed consent had been taken for the off-label application of hepatocyte-specific contrast agents from every patient before the MRI examinations. The records of our radiology department were reviewed for patients with multiple FNH-like lesions, who underwent liver MRI using hepatocyte-specific contrast agent in the last 14 years (2004–2018). The inclusion criteria were development of new liver lesions diagnosed as FNH-like nodule on MRI, presence of clinical/imaging follow-up, life expectancy more than two years after the initial diagnosis, and the absence of liver lesions on post-treatment baseline imaging. Patients were excluded if they had only one imaging examination or less than one year of follow-up.

Sixteen patients (8 male and 8 female patients) were included in this study. Demographic features and pathologic confirmation for their primary diagnoses were recorded. Liver MRI findings and active imaging follow-up with MRI were listed.

The following clinical features were assessed and recorded: primary diagnosis, age at initial diagnosis, time interval between initial diagnosis and detection of the hepatic nodule, medical treatment (including chemotherapy and radiation therapy), liver function/serological tests, presence of hematopoietic stem cell transplantation, history of veno-occlusive and/or hepatic graft versus host disease, liver biopsy results, and follow-up.

Main points

- Focal nodular hyperplasia (FNH)-like nodule refers to various regenerative nodules dispersed throughout the liver. They can mimic metastases in cancer patients who received chemotherapy.
- Liver MRI using hepatocyte-specific contrast agents appears to be a useful imaging method for the diagnosis of FNH-like lesions.
- Awareness of the typical MRI findings of these lesions avoids unnecessary biopsy in pediatric patients.

MRI technique

MRI was performed on 1.5 T imaging units using eight-channel phased-array body coil. The imaging protocol of the liver included breath-hold coronal TRUE-FISP, axial T2-weighted half-Fourier acquisition single-shot turbo spin echo, axial in- and opposed-phase chemical shift imaging, breath-hold T2-weighted fast spin-echo with fat suppression and 3D T1-weighted gradient-recalled echo fat-suppressed sequences before and after injection of the contrast agent. Table 1 summarizes the sequence parameters. Gd-EOB-DTPA (Primovist/Eovist, Bayer HealthCare Pharmaceuticals; in use since 2011) was administered to 13 patients and Gd-BOPTA (Multihance, Bracco Diagnostics) was administered to three patients. Diffusion-weighted imaging (DWI) was used to acquire single-shot echo planar images (under free breathing) with b values of 50, 400 and 800 s/mm^2.

The images were acquired in accordance with delayed hepatobiliary phase imaging at 20 minutes for Gd-EOB-DTPA and at 60 minutes for Gd-BOPTA. Intravenous boluses of contrast agents (Gd-EOB-DTPA, 0.1 mL/kg; Gd-BOPTA, 0.2 mL/kg) were infused at 1 mL/s.

Image analysis

One pediatric radiologist and an abdominal radiologist reviewed the images in consensus. A lesion was considered as a FNH-like nodule in the presence all of the following features: isointensity-to-hypointensity on T1-weighted images, isointensity-to-hyperintensity on T2-weighted images, homogeneous enhancement on arterial phase images, isointensity-to-hyperintensity on portal venous phase images and isointensity-to-hyperintensity on hepatobiliary phase images. Nodules were evaluated for size, number, contour, arterial-portal-equilibrium phase enhancement, signal intensity on T1- and T2-weighted images, hepatobiliary phase enhancement, presence of central scar (defined as central stellate area of hypointensity on T1-weighted images and hyperintensity on T2-weighted images with lack of enhancement on hepatobiliary phase), presence of ring enhancement on hepatobiliary phase (360° ring-shaped appearance of gadolinium enhancement surrounding a central area of low intensity), presence of necrotic

Table 2. The clinical findings of the patients

Patient	Sex	Primary diagnosis	Age at diagnosis of initial disease (years)	Time interval between initial diagnosis and detection of the hepatic nodule (years)	Chemotherapy drugs	Liver biopsy	Follow-up (years)	Hepatic lesion at the time of diagnosis
1	M	Rhabdomyosarcoma	16	2	VC	No	4	No
2	M	Hodgkin lymphoma	3	14	ABVD	No	14	No
3	F	Neuroblastoma	4	3	A3-A5	No	5	No
4	M	Wilms tumor	1	13	VAD	No	14	No
5	F	Neuroblastoma	5	5	A9-A11, ICE	No	7	No
6	F	Adrenocortical carcinoma	17	2	Mitotane	No	5	No
7	M	Ganglioneuroblastoma	7	9	N5, N6	No	11	No
8	F	Neuroblastoma	2 mo	2	A3-A5	No	4	Yes
9	M	Wilms tumor	4	2	VAD	No	4	No
10	F	Medulloblastoma	4	5	Temozolamide	No	7	No
11	F	Non-Hodgkin lymphoma	13	4	COPADM, CYM	No	6	No
12	F	Ganglioneuroma	6	8	A3-A5	No	11	No
13	M	Yolk sac tumor	1	10	BEP	No	14	No
14	F	Wilms tumor	6	5	VAD	No	11	No
15	M	Neuroblastoma	2	10	A3-A5	No	12	No
16	M	PNET	8	5	CACV	No	8	No

M, male; F, female; mo, months old; PNET, primitive neuroectodermal tumor ; VC, vincristine, cyclophosphamide; ABVD, adriamycin bleomycin vinblastine dacarbazine; A3, vincristine ifosfamide dacarbazine adriamycin mesna; A5, cisplatin cyclophosphamide etoposide mesna; VAD, vincristine actinomycin-D; A9, vincristine dacarbazine ifosfamide adriamycin; A11, cyclophosphamide etoposide cisplatin; ICE, ifosfamide carboplatin etoposide; N5, cisplatin/etopiside/vindesine; N6, vincristine/dacarbacin/ifosfamide/adriamycin; COPADM, cyclophosphamide vincristine prednisolone adriamycin methotrexate; CYM, cytarabine methotrexate; BEP, bleomycin etoposide cisplatin; CACV, cisplatin adriamycin cyclophosphamide vincristine.

or cystic component, hemorrhage and steatosis in the nodule, DWI signal intensity (restricted or not). During follow-up with MRI, lesions were evaluated for alteration in number, appearance and size.

Results

Table 2 summarizes clinical findings of the patients. The initial diagnoses were neuroblastoma (n=4), Wilms tumor (n=3), rhabdomyosarcoma (n=1), Hodgkin lymphoma (n=1), non-Hodgkin lymphoma (n=1), adrenocortical carcinoma (n=1), ganglioneuroblastoma (n=1), medulloblastoma (n=1), ganglioneuroma (n=1), yolk sac tumor (n=1), and primitive neuroectodermal tumor (PNET) (n=1). Age at primary tumor diagnosis ranged between 2 months and 16 years (median, 4.5 years).

All patients had received chemotherapy. Radiotherapy was administered to eight patients (total body irradiation alone in one patient, local abdominal radiotherapy in six patients and craniospinal irradiation in one patient). Only one patient had liver metastases during the diagnosis (patient number 8) and follow-up. None of the patients had developed veno-occlusive disease or had a history of hepatic graft versus host disease and hematopoietic stem cell transplantation. The time interval between the diagnosis of primary disease and the initial detection of hepatic nodules was 2–14 years (median, 5 years). At the time of hepatic nodule detection, serological and liver function tests were normal in all patients.

Table 3 summarizes imaging features of the patients. While three patients (18.7%) had a single lesion, 13 patients (81.2%) had multiple nodules. The median size of the largest nodules was 19.5 mm (range, 8–41 mm). All nodules had smooth contours. Signal intensity of the nodules was isointense (n=14) and mildly hypointense (n=2) on T1-weighted images; mildly hyperintense (n=8) and isointense (n=8) on T2-weighted images. All lesions (n=16) were hyperenhancing during the arterial phase and hyperenhancing (n=10) or isoenhancing (n=6) during the portal venous phase. On hepatobiliary phase, all lesions (n=16) appeared either hyper- or isointense compared with the surrounding liver parenchyma. Central scar (which was seen as hypointense on T1-weighted images and hyperintense on T2-weighted images with lack of enhancement on hepatobiliary phase) was detected in two patients (12.5%). Ring enhancement pattern was seen in six patients (37.5%) on hepatobiliary phase (Fig. 1). None of the nodules had hemorrhage, cystic or necrotic component or intralesional fat.

In five patients, nodules showed diffusion restriction on DWI (Fig. 2). Apparent diffusion coefficient (ADC, expressed in mm^2/s) values varied as 1.01–1.04 $\times 10^{-3}$ mm^2/s for nodules and 1.14–1.28 $\times 10^{-3}$ mm^2/s for normal liver parenchyma.

Follow-up images were available for all patients, within a total duration of 4–14 years and repeat intervals of 4–12 months. While we observed lesion growth in two patients (12.5%), increased number and size of the lesions were seen in two other patients (12.5%) (Figs. 3, 4). The nodules showed growth in the range of 6–15 mm. The mean time interval for reaching the largest size (15 mm) was 29 months (range, 6–48 months). The lesions remained stable in the follow-up period after the initial size increase.

Table 3. Imaging findings of the patients

Patient	Hepatocyte specific agent	Number of nodules	Largest nodule (mm)	T1W	T2W	Arterial phase	Portal phase	Delayed phase	Hepato-biliary phase	Central scar present	Ring enhance-ment	DWI restriction	Follow-up nodules
1	Gd-EOB-DTPA	2	8	Isointense	Iso-intense	Hyper-intense	Hyper-intense	Hyper-intense	Hyper-intense	No	No	No	Stable
2	Gd-EOB-DTPA	2	21	Isointense	Mild hyper-intense	Hyper-intense	Iso-intense	Iso-intense	Hyper-intense	No	Yes	No	Stable
3	Gd-EOB-DTPA	1	12	Isointense	Iso-intense	Hyper-intense	Iso-intense	Iso-intense	Hyper-intense	No	No	No	Stable
4	Gd-EOB-DTPA	2	28	Isointense	Mild hyper-intense	Hyper-intense	Iso-intense	Iso-intense	Hyper-intense	No	Yes	Yes	Stable
5	Gd-EOB-DTPA	2	15	Mild hypo- in-tense	Mild hyper-intense	Hyper-intense	Iso-intense	Hyper-intense	Iso-intense	Yes	Yes	Yes	Stable
6	Gd-EOB-DTPA	1	8	Isointense	Iso-intense	Hyper-intense	Hyper-intense	Hyper-intense	Hyper-intense	No	No	No	Stable
7	Gd-BOPTA	10	28	Isointense	Mild hyper-intense	Hyper-intense	Hyper-intense	Hyper-intense	Iso-intense	No	No	No	Stable
8	Gd-EOB-DTPA	>20	11	Isointense	Mild hyper-intense	Hyper-intense	Iso-intense	Iso-intense	Hyper-intense	No	No	No	Number and size increase
9	Gd-EOB-DTPA	3	11	Isointense	Iso-intense	Hyper-intense	Hyper-intense	Iso-intense	Hyper-intense	No	No	No	Size increase
10	Gd-EOB-DTPA	>20	25	Isointense	Mild hyper-intense	Hyper-intense	Hyper-intense	Hyper-intense	Hyper-intense	No	Yes	Yes	Stable
11	Gd-EOB-DTPA	2	30	Isointense	Iso-intense	Hyper-intense	Hyper-intense	Hyper-intense	Hyper-intense	Yes	Yes	No	Size increase
12	Gd-BOPTA	1	10	Isointense	Iso-intense	Hyper-intense	Hyper-intense	Hyper-intense	Iso-intense	No	No	No	Stable
13	Gd-EOB-DTPA	10	30	Isointense	Mild hyper-intense	Hyper-intense	Hyper-intense	Hyper-intense	Hyper-intense	No	Yes	No	Stable
14	Gd-EOB-DTPA	3	18	Isointense	Iso-intense	Hyper-intense	Iso-intense	Iso-intense	Iso-intense	No	No	No	Stable
15	Gd-BOPTA	13	41	Isointense	Mild hyper-intense	Hyper-intense	Hyper-intense	Hyper-intense	Hyper-intense	No	No	Yes	Stable
16	Gd-EOB-DTPA	5	25	Mild hypo-intense	Iso-intense	Hyper-intense	Hyper-intense	Hyper-intense	Iso-intense	No	No	Yes	Number and size increase

T1W, T1-weighted; T2W, T2 weighted; DWI, diffusion-weighted imaging; Gd-EOB-DTPA, gadoxetate disodium; Gd-BOPTA, gadobenate dimeglumine.

Discussion

Our study demonstrated that FNH-like lesions show iso- or hyperintensity on hepatobiliary phase images and all hepatic nodules show strong arterial enhancement Lesion growth or development of new nodules were observed in 25% of patients during follow-up.

Several types of benign vascular hepatocellular nodules have been described in the literature. These nodules are classified based on two criteria: the cell type within the nodules (regenerative or dysplastic) and the anatomic characteristics of the adjacent hepatic stroma (4). There are two main different types of nodular lesions that have been described with the history of damaged liver circulation: nodular regenerative hyperplasia and large regenerative nodules. FNH-like nodules have also been described (20). The term nodular regenerative hyperplasia is defined as multiple regenerative hepatic nodules (measuring approximately 1 mm in diameter) that involve most of the liver, which is not fibrotic/cirrhotic. The large regenerative nodules were described as nodules typically measuring 0.5–5 cm on CT or MRI in patients with Budd-Chiari syndrome (20–22).

FNH-like nodule is described as various regenerative nodules dispersed throughout the liver. The exact pathogenesis of

these nodules is unknown; however, the most widely accepted theory is associated with abnormalities of portal hepatic blood flow that, in turn, cause hepatocyte atrophy with adaptive hyperplastic reaction of hepatocytes. Diffuse hepatic vasculopathy might be the underlying mechanism for the development of multiple FNH-like lesions, particularly in cancer patients who received chemotherapy. Furlan et al. (23) reported that sinusoidal obstruction syndrome related to local defect in hepatic perfusion is suggested as the reason for development of nodular regenerative hyperplasia, which may also be responsible for the formation of FNH in patients receiving oxaliplatin based chemotherapy. FNH-like nodule may also develop due to many other conditions including chronic liver disease, vascular disorders such as portal vein congenital abnormalities, cavernous transformation of the portal vein, as well as in patients undergoing Fontan surgery (24–29). FNH-like nodule may also be seen in noncirrhotic intrahepatic portal hypertension. Possible mechanisms are portal venopathy (pre-sinusoidal component) and compression of sinusoids by the regenerative nodules (sinusoidal component) (11). These lesions can also be seen in cirrhotic liver and they should be considered in the differential diagnosis of hepatocellular carcinoma (30).

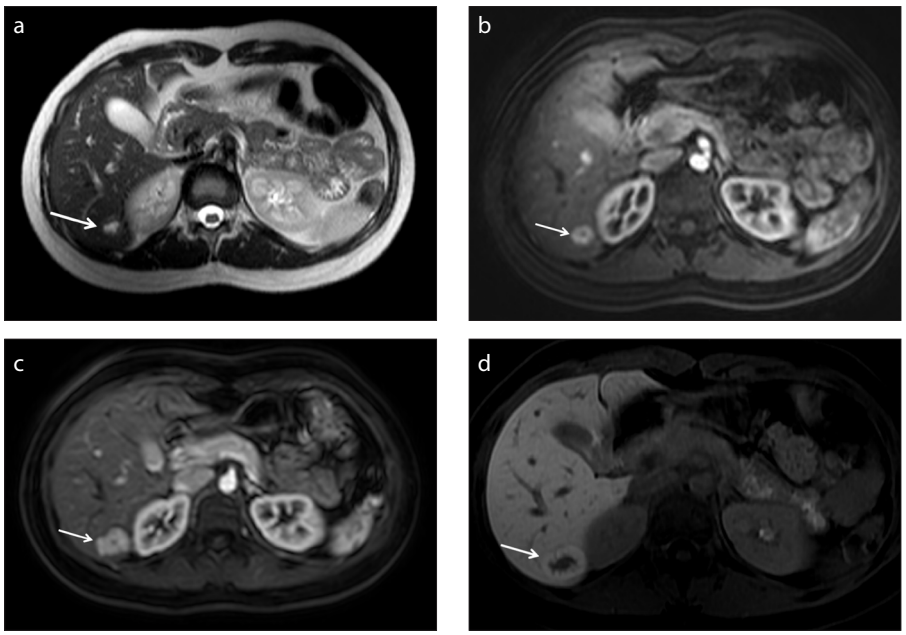

Figure 1. a–d. A 17-year-old girl with history of non-Hodgkin lymphoma. T2-weighted axial image **(a)** shows centrally hyperintense nodule in liver segment VI *(arrow)*. On dynamic studies, lesion shows strong arterial enhancement during arterial phase (**b,** *arrow*). Gadoxetate disodium-enhanced MRI **(c, d)** performed 12 months later reveals lesion growth *(arrow)*. Nodule appears hyperenhancing on arterial phase (**c,** *arrow*) and hyperintense (ring enhancement) on hepatobiliary phase (**d,** *arrow*).

Benign liver nodules after chemotherapy are mostly reported in patients who received platinum-based drugs and they encompass a spectrum of FNH, micronodular and macronodular FNH-like lesions (23, 31). Other particular drugs known to induce FNH-like nodules include thiopurines, busulfan, melphalan, thioguanine, and cyclophosphamide (18, 32). They may cause FNH-like nodules by causing damage to the endothelial cells of small hepatic veins. Our patients had received different types of chemotherapeutic agents for treatment. Neuroblastoma was the most common diagnosis and the treatment protocols comprised vincristine, cisplatin, and cyclophosphamide. In our study, the median time between the initial diagno-

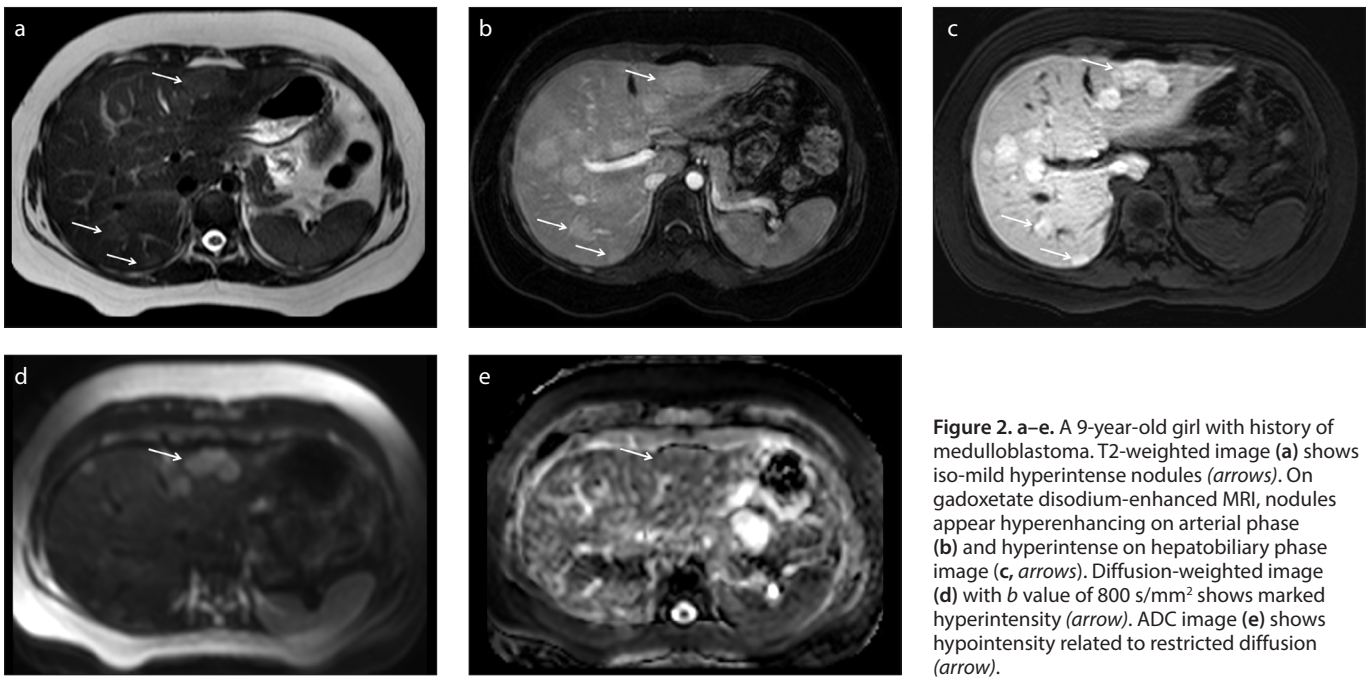

Figure 2. a–e. A 9-year-old girl with history of medulloblastoma. T2-weighted image **(a)** shows iso-mild hyperintense nodules *(arrows)*. On gadoxetate disodium-enhanced MRI, nodules appear hyperenhancing on arterial phase **(b)** and hyperintense on hepatobiliary phase image (**c,** *arrows*). Diffusion-weighted image **(d)** with *b* value of 800 s/mm^2 shows marked hyperintensity *(arrow)*. ADC image **(e)** shows hypointensity related to restricted diffusion *(arrow)*.

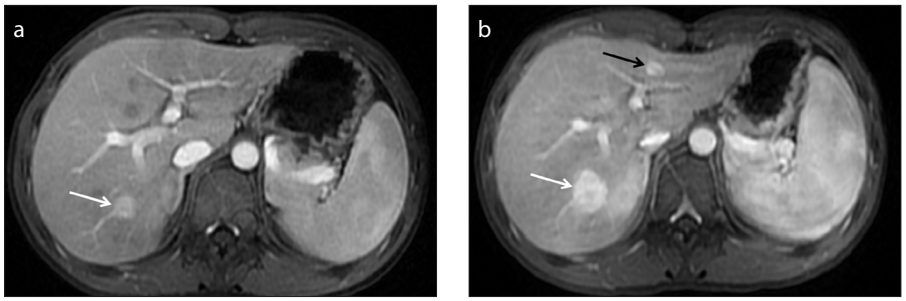

Figure 3. a, b. A 13-year-old boy with history of primitive neuroectodermal tumor. Dynamic studies show hyperenhancing nodule in segment VI on arterial phase (**a,** *arrow*). Gadoxetate disodium-enhanced MRI performed 12 months later **(b)** shows a new lesion that is hyperintense on arterial phase image *(black arrow)*. Note the growth of the nodule in segment VI *(white arrow)*.

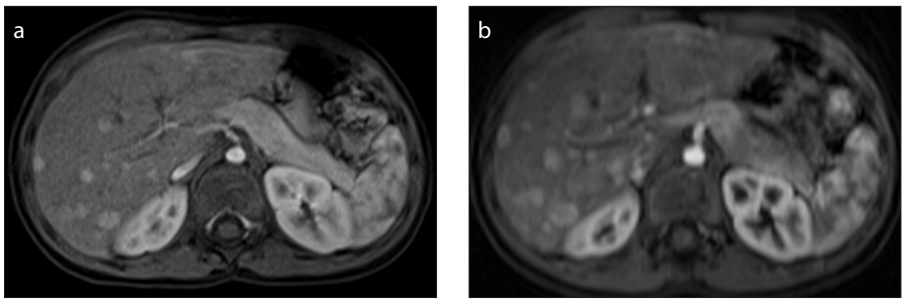

Figure 4. a, b. A 3-year-old boy with history of neuroblastoma. Gadoxetate disodium-enhanced MRI **(a)** shows strong arterial enhancement in the nodules on arterial phase. Gadoxetate disodium-enhanced MRI performed 12 months later **(b)** reveals growth of the lesions on the arterial phase.

sis and the onset of new hepatic FNH-like lesion was 5 years (range, 2–14). Likewise, long time interval has been reported for pediatric and adult patients in the literature (12, 23).

In this study, FNH-like nodules showed iso- or hyperintensity on hepatobiliary phase and were mostly isointense on T1-weighted images, mildly hyperintense on T2-weighted images. All lesions demonstrated strong arterial enhancement without washout, similar to the previous reports (12). According to Yoneda et al. (33), FNH-like nodules show iso- or hyperintensity in the hepatobiliary phase with equal or stronger organic anion transporter polypeptide (OATP8) expression compared to the surrounding liver. They also found significant correlation between OATP8 expression grade and signal intensity in the hepatobiliary phase, i.e., indicating Gd-EOB-DTPA uptake by OATP8. As a pitfall, Choi et al. (27) described FNH and FNH-like nodules that demonstrated washout on portal or delayed venous phase on dynamic CT or MRI in 10 of 84 cases including cirrhotic patients. Those nodules can be differentiated from metastases by MRI using hepatocyte-specific contrast agents (34).

Furlan et al. (23) reported lesion growth and occurrence of new FNH-like nodules during follow-up. In our study, the nodules increased both in number and size in four patients. Accordingly, we suggest that if pediatric cancer patients have imaging follow-up for their primary disease, it has to be kept in mind that these benign liver lesions may grow in size and number alike.

This study has one major limitation. None of the patients had histopathological evaluation of the nodules; biopsy was considered to be inappropriate due to typical MRI findings and benign appearance of the lesions during follow-up.

In conclusion, liver MRI using hepatocyte-specific contrast agents appears to be a useful imaging method for the diagnosis of FNH-like lesions. Hyperintensity or isointensity of the nodules on hepatobiliary phase imaging can be helpful for their diagnosis, as well as their differential diagnosis from metastases. Typical MRI findings of these lesions may avoid unnecessary biopsy in these patients. Last but not least, it should also be kept in mind that FNH-like lesions can increase in size and number during the follow-up.

Conflict of interest disclosure

The authors declared no conflicts of interest.

References

1. Grazioli L, Morana G, Kirchin MA, Schneider G. Accurate differentiation of focal nodular hyperplasia from hepatic adenoma at gadobenate dimeglumine-enhanced MR imaging: prospective study. Radiology 2005; 236:166–177. [Crossref]
2. Morana G, Grazioli L, Kirchin MA, et al. Solid hypervascular liver lesions: accurate identification of true benign lesions on enhanced dynamic and hepatobiliary phase magnetic resonance imaging after gadobenate dimeglumine administration. Invest Radiol 2011; 46:225–239. [Crossref]
3. Nakanuma Y, Hoso M, Sasaki M, et al. Histopathology of the liver in non-cirrhotic portal hypertension of unknown etiology. Histopathology 1996; 28:195–204. [Crossref]
4. Wanless IR. Micronodular transformation of (nodular regenerative hyperplasia) of the liver: a report of 64 cases among 2500 autopsies and a new classification of benign hepatocellular nodules. Hepatology 1990; 11:787–797. [Crossref]
5. Hartleb M, Gutkowski K, Milkiewicz P. Nodular regenerative hyperplasia: evolving concepts on underdiagnosed cause of portal hypertension. Word J Gastroenterol 2011; 17:1400–1409. [Crossref]
6. Libbrecht L, Cassiman D, Verslype C, et al. Clinicopathological features of focal nodular hyperplasia-like nodules in 130 cirrhotic explant livers. Am J Gastroenterol 2006; 101:2341–2346.
7. Al-Mukhaizeem KA, Rosenberg A, Sherker AH. Nodular regenerative hyperplasia of the liver: an under-recognized cause of portal hypertension in hematological disorders. Am J Hematol 2004; 75:225–230. [Crossref]
8. Seksik P, Mary JV, Beaugerie L, et al. Incidence of nodular regenerative hyperplasia in inflammatory bowel disease patients treated with azathioprine. Inflamm Bowel Dis 2011; 17:565–572. [Crossref]
9. Nakanuma Y. Nodular regenerative hyperplasia of the liver: retrospective survey in autopsy series. J Clin Gastroenterol 1990; 12:460–465. [Crossref]
10. Morris-Stiff G, White AD, Gomez D, et al. Nodular regenerative hyperplasia (NRH) complicating oxaliplatin chemotherapy in patients undergoing resection of colorectal liver metastases. Eur J Surg Oncol 2014; 40:1016–1020. [Crossref]
11. Bissonnette J, Généreux A, Côté J, et al. Hepatic hemodynamics in 24 patients with nodular regenerative hyperplasia and symptomatic portal hypertension. J Gastroenterol Hepatol 2012; 27:1336–1340. [Crossref]
12. Yoo SY, Kim JH, Eo H, Jeon TY, Sung KW, Kim HS. Dynamic MRI findings and clinical features of benign hypervascular hepatic nodules in childhood-cancer survivors. AJR Am J Roentgenol 2013; 201:178–184. [Crossref]
13. Cha DI, Yoo SY, Kim JH, Jeon TY, Eo H. Clinical and imaging findings of focal nodular hyperplasia in children. AJR Am J Roentgenol 2014; 202:960–965. [Crossref]
14. Towbin AJ, Luo GG, Yin H, Mo JQ. Focal nodular hyperplasia in children, adolescents, and young adults. Pediatr Radiol 2011; 41:341–349. [Crossref]
15. Smith EA, Salisbury S, Martin R, Towbin AJ. Incidence and etiology of new liver lesions in pediatric patients previously treated for malignancy. AJR Am J Roentgenol 2012; 199:186–191. [Crossref]

16. Bouyn CI, Leclere J, Raimondo G, et al. Hepatic focal nodular hyperplasia in children previously treated for a solid tumor: incidence, risk factors, and outcome. Cancer 2003; 97:3107–3113. [Crossref]
17. Joyner BL Jr, Levin TL, Goyal RK, Newman B. Focal nodular hyperplasia of the liver: a sequela of tumor therapy. Pediatr Radiol 2005; 35:1234–1239. [Crossref]
18. Marabelle A, Campagne D, Déchelotte P, Chipponi J, Deméocq F, Kanold J. Focal nodular hyperplasia of the liver in patients previously treated for pediatric neoplastic diseases. J Pediatr Hematol Oncol 2008; 30:546–549. [Crossref]
19. Towbin AJ, Luo GG, Yin H, Mo JQ. Focal nodular hyperplasia in children, adolescents, and young adults. Pediatr Radiol 2011; 41:341–349. [Crossref]
20. Newerla C, Schaeffer F, Terracciano L, Hohmann J. Multiple FNH-like lesions in a patient with chronic Budd-Chiari syndrome: Gd-EOB-enhanced MRI and BR1 CEUS findings. Case Rep Radiol 2012; 685486. [Crossref]
21. Brancatelli G, Federle MP, Grazioli L, Golfieri R, Lencioni R. Large regenerative nodules in Budd-Chiari syndrome and other vascular disorders of the liver: CT and MR imaging findings with clinicopathologic correlation. AJR Am J Roentgenol 2002; 178:877–883. [Crossref]
22. Ames JT, Federle MP, Chopra K. Distinguishing clinical and imaging features of nodular regenerative hyperplasia and large regenerative nodules of the liver. Clin Radiol 2009; 64:1190–1195. [Crossref]
23. Furlan A, Brancatelli G, Dioguardi Burgio M, et al. Focal nodular hyperplasia after treatment with oxaliplatin: a multi-institutional series of cases diagnosed at MRI. AJR Am J Roentgenol 2018; 210:775–779. [Crossref]
24. Marin D, Galluzzo A, Plessier A, Brancatelli G, Valla D, Vilgrain V. Focal nodular hyperplasia-like lesions in patients with cavernous transformation of the portal vein: prevalence, MR findings and natural history. Eur Radiol 2011; 21:2074–2082. [Crossref]
25. Lee YH, Kim SH, Cho MY, Shim KY, Kim MS. Focal nodular hyperplasia-like nodules in alcoholic liver cirrhosis: radiologic-pathologic correlation. AJR Am J Roentgenol 2007; 188:W459–463. [Crossref]
26. Kim MJ, Rhee HJ, Jeong HT. Hyperintense lesions on gadoxetate disodium-enhanced hepatobiliary phase imaging. AJR Am J Roentgenol 2012; 199:W575–586. [Crossref]
27. Choi JY, Lee HC, Yim JH, et al. Focal nodular hyperplasia or focal nodular hyperplasia-like lesions of the liver: a special emphasis on diagnosis. J Gastroenterol Hepatol 2011; 26:1004–1009. [Crossref]
28. Galia M, Taibbi A, Marin D, et al. Focal lesions in cirrhotic liver: what else beyond hepatocellular carcinoma? Diagn Interv Radiol 2014; 20:222–228. [Crossref]
29. Wells ML, Hough DM, Fidler JL, Kamath PS, Poterucha JT, Venkatesh SK. Benign nodules in post-Fontan livers can show imaging features considered diagnostic for hepatocellular carcinoma. Abdom Radiol (NY) 2017;42:2623–2631. [Crossref]
30. Quaglia A, Tibballs J, Grasso A, et al. Focal nodular hyperplasia-like areas in cirrhosis. Histopathology 2003; 42:14–21. [Crossref]
31. Ünal E, Karaosmanoğlu AD, Ozmen MN, Akata D, Karcaaltincaba M. Hepatobiliary phase liver MR imaging findings after Oxaliplatin-based chemotherapy in cancer patients. Abdom Radiol (NY) 2018; 43:2321–2328. [Crossref]
32. Donadon M, Di Tommaso L, Roncalli M, Torzilli G. Multiple focal nodular hyperplasias induced by oxaliplatin-based chemotherapy. World J Hepatol 2013; 5:340–344. [Crossref]
33. Yoneda N, Matsui O, Kitao A, et al. Hepatocyte transporter expression in FNH and FNH-like nodule: correlation with signal intensity on gadoxetic acid enhanced magnetic resonance images. Jpn J Radiol 2012; 30:499–508. [Crossref]
34. Karaosmanoglu AD, Onur MR, Ozmen MN, Akata D, Karcaaltincaba M. Magnetic resonance imaging of liver metastasis. Semin Ultrasound CT MR 2016; 37:533–548 [Crossref]